IEEE Access
Multidisciplinary | Rapid Review | Open Access Journal

SPECIAL SECTION ON ROADMAP TO 5G: RISING TO THE CHALLENGE

Received April 3, 2019, accepted April 25, 2019, date of publication May 2, 2019, date of current version May 23, 2019.

Digital Object Identifier 10.1109/ACCESS.2019.2914506

Channel Tracking and Transmission Design in 5G Large-Scale MIMO System

YANG WANG, YONGXUE WANG, SHENGYU ZHANG, AND HONGJIE CEN
School of Electronic and Communication Engineering, Shenzhen Polytechnic, Shenzhen 518055, China

Corresponding author: Yang Wang (wyang@ szpt.edu.cn)

This work was supported in part by the Guangdong IIOT(M-S) Engineering Technology Center under Grant 20151487, in part by the Guangdong IIOT Control Technology Engineering Laboratory under Grant 20183149, and in part by the Shenzhen IIOT Engineering Laboratory under Grant 2017823.

ABSTRACT The 5G wireless channel in the high-speed rail scene has the characteristics of fast time-varying and double selection, that is, frequency selectivity and time selectivity. The change in the instantaneous channel parameters is much faster than that in the cellular cell scene, so it is more difficult to obtain and track the instantaneous channel. This paper first researches the time and spatial correlation of the channel in 5G large-scale MIMO system and proposes a channel tracking scheme to conduct wave velocity training. Based on the predicted channel information, this paper proposes a complete downlink transmission scheme, which effectively balances 5G system resource overhead and channel tracking performance.

INDEX TERMS Channel tracking, channel transmission, spatial correlation, large-scale MIMO, high-speed rail.

I. INTRODUCTION

With the maturity of HSR construction, the demand for wireless communication in HSR has attracted wide attention at home and abroad. So far, most researches on HSR wireless communication system have attempted to adopt MIMO technology to improve the system communication performance by diversity and multiplexing gain, so as to meet passengers' needs of network activities. Large-scale MIMO is one of the symbols of 5G. The use of large-scale MIMO technology in HSR wireless communication system has become a hot research direction, because it is feasible to configure large-scale antenna if the base station and train are long enough. Based on the linear topology theory of HSR system, MIMO technology can be combined with distributed antenna system (DAS) [1], so we believe that it is a very important issue in the research on HSR wireless communication system to further improve the performance of HSR wireless communication system by applying large-scale MIMO technology.

In recent years, HSR wireless communication technology has been greatly developed. The common wireless communication scheme cannot provide high-bandwidth and low-latency service for HSR wireless system because HSR carriage has a large penetration loss. With regard to penetration loss, some scholars have proposed a two-tier architecture scheme [1], [2], that is, antenna terminal equipment is set up on the roof of the train, and users in the carriage communicate with the base station indirectly through roof antenna. We focus on the return travel between base station and terminal equipment, while the communication between terminal and user may be achieved through Wi-Fi and other protocols. Distributed antenna system (DAS) applied in HSR wireless system can reduce the transmission distance. The cell switch and radio over fiber (RoF) in DAS system and other concrete realization issues have been researched [1]. With regard to channel modeling in HSR, the expression of channel response was given in [3] and [4] combined with geological location, speed and other information, while some wireless channel parameters and channel characteristics in HSR were measured in [7]. The common HSR viaduct and plain and other scenes have been measured, and the data shows that HSR channel is composed of high-power Line-of-Sight (LoS) and a small number low-power Non-Line-of-Sight (NLoS), that is, HSR wireless channel has sparse characteristics. References [5] and [6] have put forward several pre-coding schemes based on channel LoS based on this conclusion. At present, some progress has been made in instantaneous channel acquisition technology in HSR wireless system. Reference [19] has put forward the scheme for estimating Doppler shift based on the discrete Fourier

The associate editor coordinating the review of this manuscript and approving it for publication was Muhammad Imran.

transform (DFT) and phase rotation algorithm with regard to HSR large-scale MIMO wireless system.

The wireless channel in HSR scene has the characteristics of fast time-varying and double selection, that is, frequency selectivity and time selectivity. The change in instantaneous channel parameters is much faster than that in the cellular cell scene, so it is more difficult to obtain and track the instantaneous channel. When HSR wireless communication system is combined with large-scale MIMO technology, it is more difficult to obtain and track the instantaneous channel information because of the further increase in system resource overhead required for pilot frequency transmission, channel information feedback and other technology due to the increase in channel dimension. To sum up, it is not realistic to estimate instantaneous channel information in HSR large-scale MIMO system using conventional orthogonal pilot frequency training method. When the channel changes slightly, the channel tracking scheme can be used to obtain channel information and reduce resource overhead. Some prior information such as channel statistics can be used to obtain the instantaneous channel and reduce system resource overhead and complexity in [8] and [17]. Similarly, HSR large-scale MIMO system can also use some pilot information to assist in tracking the instantaneous channel, such as the second-order statistical parameters of the channel.

In HSR large-scale MIMO wireless system, it is not easy to obtain the complete channel covariance, while HSR's location information can be obtained through the advanced positioning system, and the location information can determine some channel parameters, such as subpath departure angle, path loss, propagation delay and Doppler frequency, etc. The location information can be used to improve the performance of wireless communication technology [10]. For example, adaptive modulation based on position information and orthogonal frequency-division multiple access (OFDMA) resource allocation; multi-user MIMO system uses location information to pre-select users to reduce channel feedback; use position information to predict interference intensity; the packet algorithm [8] used in the typical joint space division multiplexing (JSDM) scheme can be achieved using location information. In channel tracking, a channel acquisition scheme was proposed in [18] based on location information and pilot frequency training in HSR large-scale MIMO system, where only some antennas need to transmit pilot frequency beams, while the complete channel matrix can be estimated by location information and temporal correlation.

Nowadays, the advanced positioning system can obtain the antenna location at the top of each carriage in HSR, and then deduce the important second-order statistical channel information combined with base station and orbit information—angle of departure (AOD) of LoS, and we focus on how to make use of the pilot information to design the channel tracking scheme. the Kalman filter tracking scheme was proposed in [12] based on temporal and spatial correlation of channel, but the scheme assumes that channel covariance is invariable, which is unrealistic in the HSR wireless communication system.

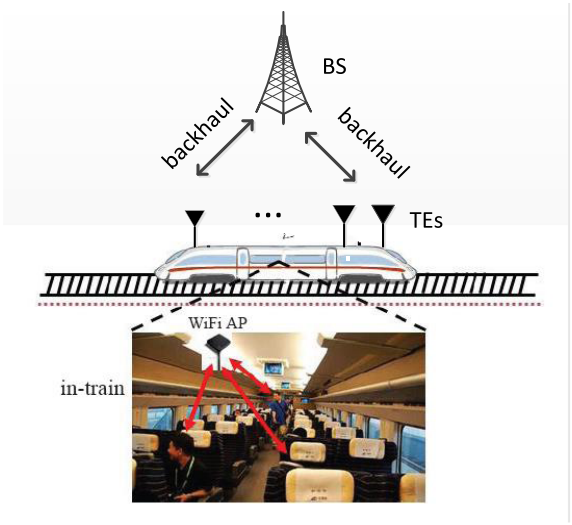

FIGURE 1. Two-tier architecture model in hsr communication.

This paper is organized as follows. In section 2, we construct the time-varying model of the channel and corresponding expression of the channel based on location information. In section 3, we design the Kalman filter tracking algorithm based on temporal and spatial correlation of channel, and discuss the design of training beam and improvement in the channel tracking scheme. In section 4, we propose a kind of less complex user grouping algorithm based on location information with regard to the multi-carriage problem, which achieves a balance between channel tracking performance and symbol resource overhead. In section 5, we give two transmission schemes based on location information and channel tracking information. In section 6, we present the simulation results to illustrate the desirable performance of the new schemes. Finally, in section 7, we give the conclusion.

II. SYSTEM AND CHANNEL MODEL

As shown in Fig. 1, this paper uses a two-tier architecture model [1], [2] which is commonly used in HSR communication scene, where the base station is distributed near the high-speed rail, and the terminal equipment (TE) is distributed at the top of the high First verify the validity of Algorithm -speed rail, responsible for the data transmission between the base station and the high-speed rail.

The main problem in this network architecture is to establish an infinite communication return between the base station and the terminal, while the communication between the terminal and the user can be achieved simply through Wi-Fi. To simplify analysis, we assume that each terminal is equipped with only one antenna, and the base station is equipped with large-scale magnitude antennas to improve the capacity and quality of wireless communication, and meet

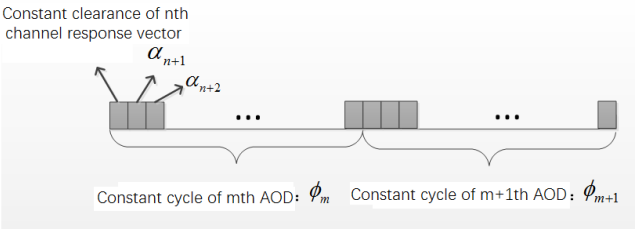

FIGURE 2. Channel frame structure diagram.

the demand for frequent access to the Internet of users in the carriage.

According to the layout characteristics of the base station in HSR scene, the channel can be modeled as LoS and NLoS, of which LoS has a higher power [3], [4], [7]. Assuming that the channel has L subpaths and the first subpath is LoS, the channel response vector from the base station to terminal k at the moment of n is expressed as:

$$\boldsymbol{h}_{k,n} = \boldsymbol{A}_t(\phi_{k,n})\boldsymbol{C}\boldsymbol{d}_{k,n} \tag{1}$$

where, $\boldsymbol{C} = diag\left(\sqrt{P}_1, \ldots, \sqrt{P}_L\right)$, P_l refers to the average power of lth path. We assume that the path power distribution of different terminals is the same, and such distribution will not vary with time on the time scale in our research. $\boldsymbol{A}_t(\phi_{k,n}) = [\boldsymbol{a}_t(\phi_{k,n,1}), \ldots, \boldsymbol{a}_t(\phi_{k,n,L}$ refers to the angle of departure (AoD) of Lth path from the base station to terminal k at the moment of n, and $\left\{\phi_{k,n,l} \,|l = 1, \ldots, L\right\}$ is corresponding to the matrix composed of antenna array response vector, respectively. Assuming the antenna is uniform linear array (ULA), the antenna array response vector is expressed as:

$$\boldsymbol{a}_t(\phi_{k,n,l}) = \left[1, e^{j\frac{2\pi}{\lambda}d\sin(\phi_{k,n,l})}, \ldots, e^{j\frac{2\pi}{\lambda}d(N_t-1)\sin(\phi_{k,n,l})}\right]^T \tag{2}$$

where, d refers to antenna distance and λ refers to wavelength. $\boldsymbol{d}_{k,n} = [\alpha_{k,n,1}, \ldots, \alpha T_{k,n,L}$ refers to $L \times 1$ vector, and $\alpha_{k,n,l} \sim \mathcal{CN}(0, 1)$ refers to the fading coefficient of lth subpath. Make $\sum_{l=1}^{L} P_l = 1$ to meet channel uniformization. It is important to note that LoS usually has a greater energy P_1 due to characteristics of HSR scene. The above-mentioned channel model reveals the spatial model structure of the channel, and here is the time-varying model of the channel.

As shown in Fig. 2, the channel is divided into several cycles because the change in the fading coefficient $\alpha_{k,n,l}$ is faster than that in subpath AOD $\phi_{k,n,l}$. Each subpath in each cycle has a constant corresponding AOD, and each cycle is composed of several time slots. The instantaneous channel response vector is constant in each time slot, the time slot is equivalent to the coherence time of channel and the fading coefficient of each path between different time slots may vary. In the channel time-varying model in [11], channel $\boldsymbol{h}_n$ and channel $\boldsymbol{h}_{n+1}$ have the following temporal

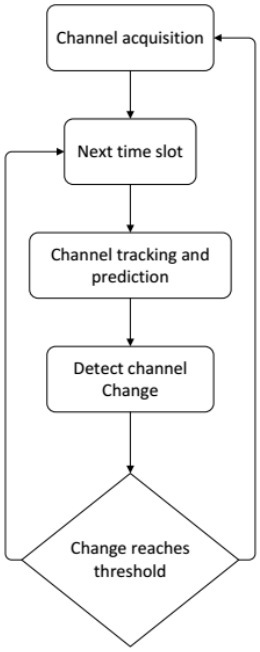

FIGURE 3. Relationship among Channel acquisition, tracking and detection.

correlation:

$$\begin{cases} \boldsymbol{h}_{k,n+1} = \boldsymbol{A}_t\left(\phi_{k,n+1}\right)\boldsymbol{C}\boldsymbol{d}_{k,n+1} \\ \boldsymbol{A}_t\left(\phi_{k,n+1}\right) = \boldsymbol{A}_t\left(\phi_{k,n} + \Delta\phi_{k,n}\right) \\ \boldsymbol{d}_{k,n+1} = \rho\boldsymbol{d}_{k,n} + \sqrt{1-\rho^2}\boldsymbol{b}_{k,n+1} \end{cases} \tag{3}$$

where, channel time-varying coefficient $\rho = E\left[\alpha_{n,i}\alpha^*_{n+1,i}\right] \in, [01], i = 1, \ldots, L$ follows $\rho = J_0(2\pi f_D T)$ of Jake's model, of which $J_0()$ refers to zero-order Bessel function, and $f_D = f_c v/c$ refers to Doppler frequency. $\boldsymbol{b}_{k,n+1} = [b_{k,n+1,1}, \ldots, b_{Tk,n+1,L}$ and $\boldsymbol{d}_{k,n}$ are independent, and $b_{k,n+1,l}$. Corresponding to Fig. 2, $\Delta\phi_{k,n} = 0$ if n and $n+1$ are in the same cycle.

III. CHANNEL TRACKING SCHEME

Given the time-varying characteristics of the channel described in Section 2 and channel acquisition scheme in [13], as shown in Fig. 3, it includes channel acquisition, tracking prediction and detection modules, and the details are as follows: to obtain channel parameters using relevant technology in the initial stage, then to track and predict the channel, to detect and predict channel quality after a period of time and need to obtain the channel once again if the difference between predicted channel and actual channel exceeds the threshold. This paper only focuses on ''Channel tracking and prediction''.

Assuming that there are $M(M = M_d + M_p)$ time slots in one cycle as shown in Fig. 2, it is different because every traditional time slot requires channel estimate. Since the initial channel information is accurate, this paper considers applying predicted channel in the first M_d time slots to precoding, scheduling and other scheme design to improve data

transmission efficient, and sending training beams in the last M_p time slots to track the channel.

A. CHANNEL TRACKING MODELING AND FEASIBLE SCHEME DISCUSSION

Based on the time-varying model of channel parameters given in (1) and (3), we can obtain the time-varying relationship of channel vector. Firstly, the channel vector of the $n+1$ time slot is shown below:

$$\begin{aligned}
&\boldsymbol{h}_{k,n+1} \\
&\quad = \boldsymbol{A}_t\left(\phi_{k,n+1}\right)\boldsymbol{C}\boldsymbol{d}_{k,n+1} \\
&\quad = \boldsymbol{A}_t(\phi_{k,n+1})\boldsymbol{C}(\rho\boldsymbol{d}_{k,n} + \sqrt{1-\rho^2}\boldsymbol{b}_{k,n+1}) \\
&\quad = \sum_{l=1}^{L}\boldsymbol{h}_{k,n+1,l} = \sum_{l=1}^{L}\sqrt{P_l}\alpha_{k,n+1,l}\boldsymbol{a}_t(\phi_{k,n+1,l}) \\
&\quad = \sum\nolimits_{l=1}^{L}\sqrt{P_l}(\rho\alpha_{k,n,l} + \sqrt{1-\rho^2}b_{k,n+1,l})\boldsymbol{a}_t(\phi_{k,n+1,l})
\end{aligned} \tag{4}$$

where, $\boldsymbol{h}_{k,n+1,l} = \sqrt{P_l}\alpha_{k,n+1,l}\boldsymbol{a}_t(\phi_{k,n+1,l})$ refers to the corresponding channel vector of the lth subpath in $n+1$ time slot, and the change in array vector is expressed using array transfer matrix $\boldsymbol{T}_{k,n,l}$ as follows:

$$\begin{aligned}
&\boldsymbol{a}_t\left(\phi_{k,n+1,l}\right) \\
&\quad = \left[1, e^{j\frac{2\pi}{\lambda}d\sin(\phi_{k,n+1,l})}, \ldots, e^{j\frac{2\pi}{\lambda}d(N_t-1)\sin(\phi_{k,n+1,l})}\right]^T \\
&\quad = \boldsymbol{T}_{k,n,l}\boldsymbol{a}_t(\phi_{k,n,l})
\end{aligned} \tag{5}$$

$$\begin{aligned}
\boldsymbol{T}_{k,n,l} = diag(&1, e^{j\frac{2\pi}{\lambda}d(\sin(\phi_{k,n+1,l})-\sin(\phi_{k,n,l}))}, \\
&\ldots, e^{j\frac{2\pi}{\lambda}d(N_t-1)(\sin(\phi_{k,n+1,l})-\sin(\phi_{k,n,l}))}),\ l=1,\ldots,L
\end{aligned} \tag{6}$$

According to (4):

$$\begin{aligned}
&\boldsymbol{h}_{k,n+1} \\
&\quad = \sum_{l=1}^{L}\sqrt{P_l}(\rho\alpha_{k,n,l} + \sqrt{1-\rho^2}b_{k,n+1,l})\boldsymbol{T}_{k,n,l}\boldsymbol{a}_t(\phi_{k,n,l}) \\
&\quad = \sum_{l=1}^{L}\rho\boldsymbol{T}_{k,n,l}\left(\sqrt{P_l}\alpha_{k,n,l}\boldsymbol{a}_t(\phi_{k,n,l})\right) + \sqrt{1-\rho^2}\boldsymbol{T}_{k,n,l} \\
&\qquad \left(\sqrt{P_l}b_{k,n+1,l}\boldsymbol{a}_t(\phi_{k,n,l})\right) \\
&\quad = \sum\nolimits_{l=1}^{L}\left(\rho\boldsymbol{T}_{k,n,l}\boldsymbol{h}_{k,n,l} + \sqrt{1-\rho^2}\boldsymbol{c}_{k,n+1,l}\right)
\end{aligned} \tag{7}$$

Corresponding vector of the channel of each subpath meets:

$$\boldsymbol{h}_{k,n+1,l} = \rho\boldsymbol{T}_{k,n,l}\boldsymbol{h}_{k,n,l} + \sqrt{1-\rho^2}\boldsymbol{c}_{k,n+1,l} \tag{8}$$

where, $\boldsymbol{h}_{k,n,l} = \sqrt{P_l}\alpha_{k,n,l}\boldsymbol{a}_t(\phi_{k,n,l})$ and $\boldsymbol{c}_{k,n+1,l} = \sqrt{P_l}b_{k,n+1,l}\boldsymbol{T}_{k,n,l}\boldsymbol{a}_t(\phi_{k,n,l}) \cong \boldsymbol{h}_{k,n+1,l}$, of which $\cong$ means that the statistical characteristics are the same, so

$$\begin{aligned}
E\left\{\boldsymbol{c}_{k,n+1,l}\boldsymbol{c}_{k,n+1,l}^H\right\} &= E\left\{\boldsymbol{h}_{k,n+1,l}\boldsymbol{h}_{k,n+1,l}^H\right\} \\
&= \boldsymbol{R}_{k,n+1,l} \\
&= P_l\boldsymbol{a}_t(\phi_{k,n+1,l})\boldsymbol{a}_t(\phi_{k,n+1,l})^H
\end{aligned} \tag{9}$$

It can be seen from (7) that there is no status transfer relationship displayed from $\boldsymbol{h}_{k,n}$ to $\boldsymbol{h}_{k,n+1}$, but such relationship can be found in every subpath according to (8). Therefore, we can deal with the tracking of channel vector in two ways. First is to approximately use LoS to replace total channel and neglect NLoS; second is to track each subpath separately. In this case, we can convert channel tracking into adaptative filtering, and we consider using Kalman filter to solve tracking problem in this paper.

B. KALMAN FILTER TRACKING

Without loss of generality, we start with the hypothesis that AOD of each subpath and its time-varying mode are known, that is, array transfer matrix $\boldsymbol{T}_{n,l}$ and array vector $\boldsymbol{a}_t(\phi_{k,n,l})$ are known, in which case each subpath can be tracked, and its status equation can be rearranged as follows:

$$\boldsymbol{h}_{k,n+1,l} = \rho\boldsymbol{T}_{k,n,l}\boldsymbol{h}_{k,n,l} + \sqrt{1-\rho^2}\boldsymbol{c}_{k,n+1,l} \tag{10}$$

Corresponding correlation matrix is shown below:

$$\boldsymbol{R}_{k,n+1,l} = \rho^2\boldsymbol{T}_{k,n,l}\boldsymbol{R}_{k,n,l}\boldsymbol{T}_{k,n,l}^H + (1-\rho^2)\boldsymbol{R}_{k,n+1,l} \tag{11}$$

The error covariance matrix in Kalman filter is shown below:

$$\boldsymbol{P}_{\frac{k,n+1,l}{k,n,l}} = \rho^2\boldsymbol{T}_{k,n,l}\boldsymbol{P}_{\frac{k,n,l}{k,n,l}}\boldsymbol{T}_{k,n,l}^H + (1-\rho^2)\boldsymbol{R}_{k,n+1,l} \tag{12}$$

Based on the said analysis, assuming that the base station in $n+1$ time slot transmits downlink training beam $\boldsymbol{s}_{k,n+1,l}$ to certain terminal, the terminal receives corresponding signal as follows:

$$y_{k,n+1,l} = \boldsymbol{s}_{k,n+1,l}^H\boldsymbol{h}_{k,n+1} + w_{k,n+1} \tag{13}$$

where, $w_{k,n+1} \sim \mathcal{CN}(0,\sigma_w^2)$ refers to the noise on the receiving end. According to (10), (12) and (13), Kalman filter algorithm is obtained as shown in Algorithm 1.

With reference to the frame structure shown in Fig. 1, $\boldsymbol{T}_{n-1,l}$ in Algorithm 1 is equal to unit matrix and degraded into the scheme in [12] when the time slot is in the same cycle with the previous time slot, that is, the channel covariance is invariable. when the time slot is at the intersection of cycle, that is, the time slot and the previous time slot are in different cycles, $\boldsymbol{T}_{n-1,l}$ is no longer the unit matrix, which can be obtained according to (6).

C. OPTIMAL PILOT FREQUENCY DESIGN

With the goal of minimizing the trace of error covariance in Algorithm 1, refer to (21). Solve the training beam $\boldsymbol{s}_{n,l}$ in Algorithm 1 using the deduction method of sequential optimal training beam in [12] and obtain Algorithm 2. The sequential optimal training beam obtained in Algorithm 2 is the main characteristic vector of the current channel covariance (that is, the characteristic vector corresponding to the maximum eigenvalue).

$$\begin{cases}
\min tr\left(\boldsymbol{P}_{\frac{n,l}{n,l}}\right) \\
s.t.\ \left\|\boldsymbol{s}_{n,l}\right\|_2^2 = \rho_p
\end{cases} \tag{21}$$

Algorithm 1 Kalman Filter Tracking Algorithm (Take lth Subpath for Example and Omit User Subscript)

While $m = 0, 1, \ldots$ do
for $n = 1$ *to* M do
if $n > M_d$ then

$$\hat{\boldsymbol{h}}_{\frac{n,l}{n-1},l} = \rho \boldsymbol{T}_{n-1,l} \hat{\boldsymbol{h}}_{\frac{n-1,l}{n-1,l}} \tag{14}$$

$$\boldsymbol{P}_{\frac{n,l}{n-1,l}} = \rho^2 \boldsymbol{T}_{n-1,l} \boldsymbol{P}_{\frac{n-1,l}{n-1,l}} \boldsymbol{T}^H_{n-1,l} + (1-\rho^2)\boldsymbol{R}_{n,l} \tag{15}$$

$$\boldsymbol{K}_{n,l} = \frac{\boldsymbol{P}_{\frac{n,l}{n-1,l}} \boldsymbol{s}_{n,l}}{\boldsymbol{s}^H_{n,l} \boldsymbol{P}_{\frac{n,l}{n-1,l}} \boldsymbol{s}_{n,l} + \sigma_w^2} \tag{16}$$

$$\hat{\boldsymbol{h}}_{\frac{n,l}{n},l} = \hat{\boldsymbol{h}}_{\frac{n,l}{n-1},l} + \boldsymbol{K}_{n,l}(y_{n,l} - \boldsymbol{s}^H_{n,l} \hat{\boldsymbol{h}}_{\frac{n,l}{n-1},l}) \tag{17}$$

$$\boldsymbol{P}_{\frac{n,l}{n,l}} = \boldsymbol{P}_{\frac{n,l}{n-1,l}} - \boldsymbol{K}_{n,l} \boldsymbol{s}^H_{n,l} \boldsymbol{P}_{\frac{n,l}{n-1,l}} \tag{18}$$

else

$$\hat{\boldsymbol{h}}_{\frac{n,l}{n},l} = \hat{\boldsymbol{h}}_{\frac{n,l}{n-1},l} = \rho \boldsymbol{T}_{n-1,l} \hat{\boldsymbol{h}}_{\frac{n-1,l}{n-1,l}} \tag{19}$$

$$\boldsymbol{P}_{\frac{n,l}{n,l}} = \boldsymbol{P}_{\frac{n,l}{n-1,l}} = \rho^2 \boldsymbol{T}_{n-1,l} \boldsymbol{P}_{\frac{n-1,l}{n-1,l}} \boldsymbol{T}^H_{n-1,l} + (1-\rho^2)\boldsymbol{R}_{n,l} \tag{20}$$

end if
end for
end while

Note that the channel in (13) is an overall channel other than a subchannel. Based on the conclusion that "sequential optimal training beam is the array response vector of the current cycle", the following formula is obtained when the number of antennas is greater:

$$\boldsymbol{s}^H_{n+1,l} \boldsymbol{h}_{n+1} \approx \boldsymbol{s}^H_{n+1,l} \boldsymbol{h}_{n+1,l} \tag{25}$$

Therefore, (13) is approximately expressed as $y_{k,n+1,l} = \boldsymbol{s}^H_{k,n+1,l} \boldsymbol{h}_{k,n+1} + w_{k,n+1} \approx \boldsymbol{s}^H_{k,n+1,l} \boldsymbol{h}_{k,n+1,l} + w_{k,n+1}$.

D. IMPROVED KALMAN FILTER TRACKING SCHEME

When using Algorithm 1 to track the instantaneous channel, L training beams shall be transmitted within a time slot, and the beams shall separately strike in the array direction of each subpath, so as to obtain L measured values. Given the actual limited number of antennas, however, the degree of approximation of (25) drops, that is, the interference of other subpaths on the measured data of target subpath cannot be neglected. For this reason, we have attempted to subtract the projection of other subpath channels in the measured value of the channel of the subpath from the measured value to improve accuracy, and the specific steps are shown in Algorithm 3.

Algorithm 2 Solution Algorithm of Sequential Optimal Pilot Frequency Sequence (Take lth Subpath for Example and Omit User Subscript)

$$\boldsymbol{u} = \frac{\boldsymbol{a}_t(\phi_{n,l})}{|\boldsymbol{a}_t(\phi_{n,l})|} \tag{22}$$

while $m = 0, 1, \ldots$ do
for $n = 1$ *to* M do

$$\boldsymbol{u} = \boldsymbol{T}_{n,l} \boldsymbol{u} \tag{23}$$

if $n > M_d$ then

$$\boldsymbol{s}_{n,l} = \sqrt{\rho_P} \boldsymbol{u} \tag{24}$$

end if
end for
end while

Algorithm 3 Improved Kalman Filter Tracking Algorithm

for $l = 1, \ldots, L$
if $l > 1$
for $p = 1$ *to* $(l-1)$

$$y_{m,l} = y_{m,l} - \boldsymbol{s}^H_{m,l} \hat{\boldsymbol{h}}_{m,p/m,p} \tag{26}$$

end for
end if
Execute Algorithm 1;
end for

E. KALMAN FILTER TRACKING FROM THE PERSPECTIVE OF LoS

The above-mentioned Kalman tracking scheme assumes that AOD of each subpath and its variation trend are known, which cannot usually be realized in practice, while it is relatively easy to obtain AOD and its variation trend of LoS. Therefore, we provide channel tracking algorithm only with the information about AOD of LoS.

1) To solve the sequential optimal training beam of LoS using Algorithm 2;

2) To track corresponding channel weight of LoS using Algorithm 1;

3) Due to higher power of LoS, to approximate overall channel using the corresponding channel of LoS.

IV. MULTI-USER GROUPING SCHEME

In section 3, we give the channel tracking scheme of single terminal. In practice, HSR carriages are configured with terminals on top, which is equivalent to the multi-user circumstance in cellular cell. This section researches how to distribute symbol resources in time slot to each terminal.

Assuming that there are K terminals, training beams shall be transmitted to a terminal within a symbol time (a time slot

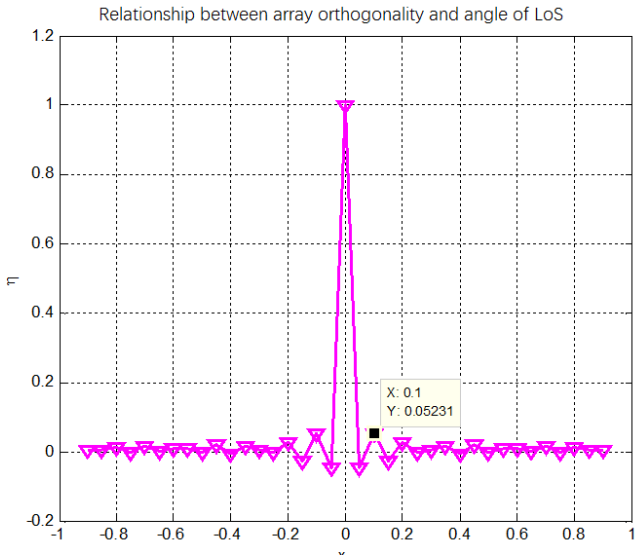

FIGURE 4. Array Correlation Coefficient and Phase Difference.

is composed of multiple symbol times) to avoid the interference between terminals, so K symbol times are needed in a time slot to complete the training of K terminals. When there are a number of terminals and the symbol resource in a time slot may be insufficient, this chapter proposes the user grouping algorithm. The main idea is to take the inner product of corresponding array response vector of LoS as correlation criterion and distribute terminals with stronger correlation into different groups to enable the terminals in the same group to have the approximate orthogonal channel, then transmit the sum of training beams of terminals in the same group within the same symbol time, which not only ensures that other beams transmitted at the same time have no greater impact on the target measured value, but saves symbol resources.

The uniform array response corresponding to (2) is shown below:

$$\boldsymbol{u}_{k,1} = \frac{1}{\sqrt{N_t}}[1, \exp(j\frac{2\pi}{\lambda}d\sin(\phi_{k,n,1})), \ldots, \exp(j\frac{2\pi}{\lambda}d\sin(\phi_{k,n,1})(N_t-1))]^T \quad (27)$$

where, $\phi_{k,n,1}$ refers to user k's AOD of LoS at the n moment. The channel correlation coefficient of terminals k and l is shown below:

$$\eta_{k,l} = \boldsymbol{u}_{k,1}^H \boldsymbol{u}_{l,1} = \sum_{n=1}^{N_t} \exp\left(j2\pi D\left(\sin\left(\theta_{l,1}\right) - \sin\left(\theta_{k,1}\right)\right)(n-1)\right) \quad (28)$$

To avoid high-dimensional vector operation, we analyze the relationship between $\eta_{k,l}$ and $x_{k,l} = \sin(\theta_{k,1}) - \sin(\theta_{l,1})$ through simulation.

As shown in Fig. 4, $\eta_{k,l} \leq 0.05231$ when $|x_{k,l}| \geq 0.1$, the array vector corresponding to TE of the two terminals is approximately orthogonal, so that the training beams of two

Algorithm 4 User Grouping Algorithm

1) User set is expressed as U;
2) Put the first user in the first group, which is expressed as G_1; the known group number is expressed as $N = 1$;
$U = U - \{1\}$;
  For $k \in U$
$flag = 1$;
  For $n = 1$ *to* N
    For $m \in G_n$
      If $x_{k,m} < 0.1$
        $flag = 0$; Break;
      End if
  End for
    If $flag = 1$
      $G_n = G_n \cup k\}$; $U = U - \{k\}$; break;
  End if
End for
if $flag = 0 || n == N$
set $G_{N+1} = \{k\}$; $N = N + 1$;
end if
end for

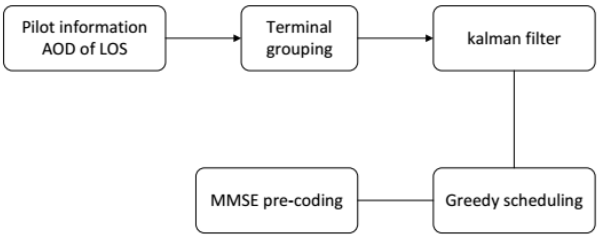

FIGURE 5. System scheme a.

users can be transmitted together, and the specific steps are shown in Algorithm 4.

V. TRANSMISSION SCHEME

Based on the tracked and predicted channel information, this paper proposes the complete transmission scheme based on location information, as shown in Fig. 5.

1) To obtain AOD and its variation information of channel LoS of each terminal through HSR control system;

2) To group all terminals using Algorithm 4;

3) To obtain the sequential optimal training beam of each terminal using Algorithm 2 during the training cycle;

4) To track the instantaneous channel using Algorithm 1 based on variation information of LoS during the training cycle;

5) To predict the instantaneous channel using Algorithm 1 during the data transmission cycle;

6) To perform greedy scheduling [17] and MMSE pre-coding using predicted channel information during the data transmission cycle.

Comparatively speaking, there is a simpler transmission scheme b that makes use of location information only, that is, AOD of LoS.

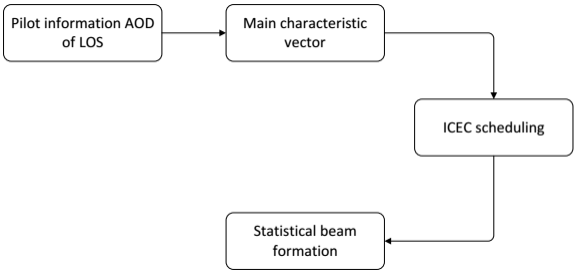

FIGURE 6. System Scheme b.

TABLE 1. Simulation parameters.

Parameter	Quantity
N_t	64
$v/(km/h)$	300
f_c/GHz	2.5
ρ_P/dB	0
L	3
$M_p/time\ slot$	5
$M_d/time\ slot$	5

1) To obtain AOD and its variation information of channel LoS of each terminal;

2) To approximate the most dominant eigenvector of channel covariance with the corresponding array vectors of LoS;

3) To select users using ICEC scheduling scheme [15];

4) To design pre-coding vector using statistical beam formation [16];

5) To obtain system traversal and rate;

The pilot information is consistent in both Scheme a and Scheme b. Scheme a tracks the instantaneous channel and obtains more channel information by increasing beam training. Combined with the pre-coding and scheduling scheme that can make full use of channel information, the system traversal and rate of Scheme a shall be higher than that of Scheme a.

VI. SIMULATION RESULT

In this section, the experiment analyzes the performance of channel tracking and transmission design scheme mentioned in this paper from the perspective of channel tracking quality of single terminal and system traversal and rate of multiple terminals.

A. CHANNEL TRACKING OF SINGLE TERMINAL

With regard to the parameter setting in [12] as shown in Table 1, the computing process of AOD of LoS is omitted in simulation, and results are obtained by performing the initial AOD $\phi_{0,1} \sim [-60°, 60°]$ of LoS of Monte-Carlo simulation. Assume that the power distribution of three subpaths is [0.80.10.1]. Based on parameters in Table 1, the time-varying parameter is calculated as $\rho = J_0(2\pi f_D T) = 0.953$.

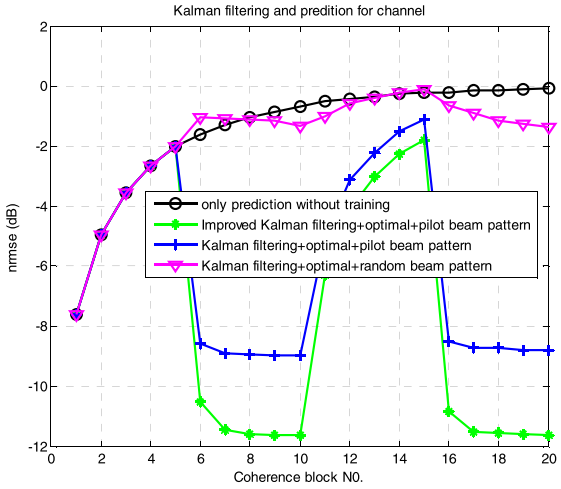

FIGURE 7. Root-mean-square error of single-terminal tracking channel.

Perform simulation analysis on Algorithms 1∼3. Assuming that AOD and its variation of L subpaths are known, perform Kalman prediction and tracking on the channel of L subpaths, and then combine into an overall channel. During training, it is required to transmit L training beams separately in each time slot within M_p time slots. The uniform root-mean-square error in simulation results shall be used to reflect the quality of tracking channel, that is:

$$nrmse_k = 20\log_{10}\left(\sqrt{\frac{1}{M}\sum_{m=1}^{M}\frac{\left\|\hat{\boldsymbol{h}}_k - \boldsymbol{h}_k\right\|_F^2}{\left\|\hat{\boldsymbol{h}}_k\right\|_F^2 \|\boldsymbol{h}_k\|_F^2}}\right)$$

where, M refers to the number of Monte-Carlo simulation, $\hat{\boldsymbol{h}}_k$ refers to the channel predicted and tracked by user k and $\boldsymbol{h}_k$ refers to the theoretical value of $\hat{\boldsymbol{h}}_k$.

Fig. 7 gives the optimal beam and random beam obtained using Algorithm 2. Combined with the channel prediction and tracking performance of Kalman filter tracking scheme in Algorithm 1 and Algorithm 3, Fig. 7 also gives the quality of predicted channel without beam training process to show the validity of the scheme mentioned in this paper. As shown in Fig. 7, the performance of channel tracking and prediction schemes given in Algorithm 1 and Algorithm 3 is higher than that without beam training, which proves the necessity of beam training and validity of Algorithm 1 and Algorithm 3 as mentioned. The quality of tracked channel in Algorithm 3 is higher than that in Algorithm 1, which proves the validity of the improved algorithm as mentioned. Compared to the random training beam, the training beam obtained using Algorithm 2 can obtain a lower root-mean-square error of channel, that is, a higher channel quality.

Through detailed analysis of the curve trend in Fig. 7, we can see that the predicted and tracked channel error becomes larger during data transmission, while sharply drops during tracking training period. However, the quality of predicted channel without training process will become worse,

TABLE 2. Simulation parameters.

Parameter	Quantity
N_t	64
$v/(km/h)$	300
f_c/GHz	2.5
ρ_P/dB	10
ρ	0.953
L	3
M	30
K	41

which proves the validity once again of Kalman filter tracking scheme mentioned in this paper.

Based on the above analysis, the predicted and tracked channel error will become larger in the time slot of data transmission, while becoming smaller with beam training after entering the time slot of beam training (during 6-10 time slots as shown in Fig. 7). However, channel error cannot be reduced limitlessly, that is, channel error will hit a local minimum after about 2-5 training sessions, which shows the rapid convergence of the channel tracking scheme mentioned in this paper.

VII. MULTI-TERMINAL SYSTEM AND RATE

With regard to the characteristics of HSR multi-terminal configuration, the multi-terminal channel tracking scheme and system transmission scheme mentioned in this paper are simulated.

Table 2 shows the simulation parameters in this section, and the power distribution of L subpaths is expressed as [0.80.10.1]. The simulation assumes that 41 terminals are distributed at the top of HSR, the initial AOD of LoS of these 41 terminals is $-60° : 3° : 60°$, respectively. Due to the greater number M of time slots during each cycle, we do 2 cycles of simulation only to ensure the quality of tracked channel, and then go back to the channel acquisition stage as shown in Fig. 3 (that is, obtain the exact channel parameters once again). The simulation results of this section are based on the assumption that there is the information about AOD of LoS of the channel only, so that simulation results are more consistent with actual conditions.

First verify the validity of Algorithm 4., Fig. 8 provides a simulation comparison of the channel tracking and prediction performance under three schemes, such as "Algorithm 4", "training beam transmitted to only one terminal in a symbol" and "sum of training beams transmitted to all terminals in a symbol". The simulation results show that Packet Algorithm 4 can approximately reduce the symbol resources required in each time slot to half of the terminal number. To highlight the variation trend, Fig. 8 shows two cycles, and each cycle is composed of 10 time slots. The first half is for data transmission and the second half is for the simulation results of beam training. Fig. 8 shows that the channel tracking quality after grouping is inferior to that of

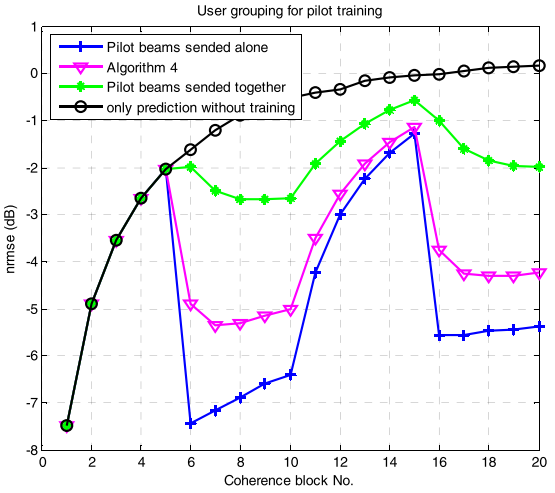

FIGURE 8. Root-mean-square error of multi-terminal tracking channel.

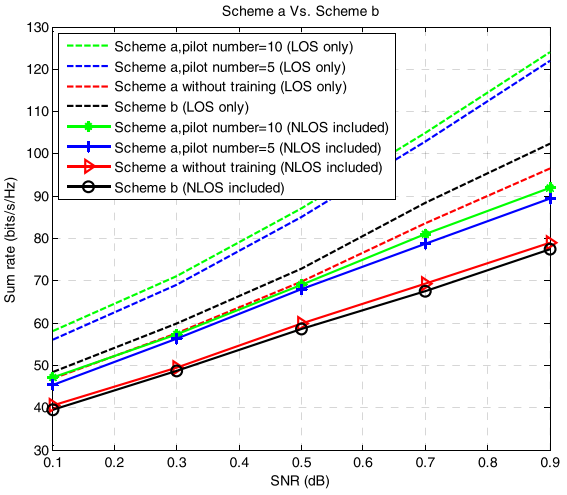

FIGURE 9. Traversal and rate of system transmission scheme a.

training beams transmitted separately to each terminal, but superior to that of the sum of training beams transmitted to all terminals, which balances the channel tracking performance and resource overhead. Fig. 8 shows that the channel tracking error can hit the local minimum after about 2-3 training sessions during the beam training cycle (during 6-10 time slots as shown in Fig. 8), while redundant pilot training can only increase the channel error.

Fig. 9 shows the system and rate obtained using Scheme a and Scheme b. Consistent with theoretical analysis, Scheme a is superior to Scheme b because Scheme a obtains the information of fading coefficient of the channel compared to Scheme b after pilot frequency training, while MMSE pre-coding and greedy scheduling can completely make use of such channel information, which proves the necessity once again of pilot frequency training in channel tracking scheme. Fig. 9 shows that the more times the pilot frequency training during each cycle, the higher the traversal and rate.

Fig. 9 also gives the system traversal and rate of Scheme A without pilot frequency training process and based on predicted channel information only.

As with the Scheme b, there is no pilot frequency training process. From Fig. 9, it can be seen that the two schemes have similar performance, but Scheme b is a transmission scheme based on statistical channel information, which is less executed than Scheme a in terms of pre-coding and scheduling algorithm. Therefore, it is more suitable for practical use in the absence of pilot frequency training process. The system performance is poor without pilot frequency training process, but the performance can still be close to the system performance with pilot frequency training process under the circumstance where there is no symbol resource overhead, indicating the importance and superiority of the use of geological location information in HSR.

Fig. 9 also simulates the results that the strength of LoS reaches the limit (channel has LoS only). As Scheme a only tracks LoS, the quality of the channel tracked in Scheme a is improved when channel has LoS only, so is traversal and rate. For Scheme b, the main characteristic vector of channel covariance in Step 2 is the corresponding array response vector of LoS, and the two are exactly the same (other than approximate), so traversal and rate will also be improved. Therefore, the traversal and rate of three curves with LoS only will be higher than corresponding curves with NLoS. It should be noted that the traversal and rate of Scheme with LoS only is higher than those in Scheme a in the absence of pilot frequency training process, indicating that Scheme B is more advantageous when the channel has LoS only.

VIII. CONCLUSION

This paper first establishes corresponding expression of the channel based on time-varying coefficient and location information of the channel, then gives Kalman filter tracking channel scheme based on temporal and spatial correlation of the channel and gives the algorithm of sequential optimal training beam according to location information. Later, this paper presents a kind of simple user grouping algorithm with regard to the typical multi-terminal configuration system, which effectively balances resource overhead and channel tracking performance. Finally, this paper proposes two complete downlink transmission schemes based on predicted channel information and performs simulation verification on the advantage of using location information in HSR wireless system and necessity of beam training.

REFERENCES

[1] J. Wang, H. Zhu, and N. J. Gomes, "Distributed antenna systems for mobile communications in high speed trains," *IEEE J. Sel. Areas Commun.*, vol. 30, no. 4, pp. 675–683, May 2012.

[2] X. Chen, J. Lu, P. Fan, and K. B. Letaief, "Massive MIMO beamforming with transmit diversity for high mobility wireless communications," *IEEE Access*, vol. 5, pp. 23032–23045, Oct. 2017.

[3] X. Chen, J. Lu, T. Li, P. Fan, and K. B. Letaief, "Directivity-beamwidth tradeoff of massive MIMO uplink beamforming for high speed train communication," *IEEE Access*, vol. 5, pp. 5936–5946, Apr. 2017.

[4] A. Ghazal, C. X. Wang, and B. Ai, "A nonstationary wideband MIMO channel model for high-mobility intelligent transportation systems," *IEEE Trans. Intell. Transp. Syst.*, vol. 16, no. 2, pp. 885–897, Apr. 2015.

[5] M. Cheng and X. Fang, "Location information-assisted opportunistic beamforming in LTE system for high-speed railway," *Eurasip J. Wireless Commun. Netw.*, vol. 1, no. 1, pp. 1–7, Jul. 2012.

[6] T. Zhou, C. Tao, and L. Liu, "High-speed railway channel measurements and characterizations: A review," *J. Modern Transp.*, vol. 20, no. 4, pp. 199–205, Dec. 2012.

[7] A. Adhikary and G. Caire, "Joint spatial division and multiplexing: Opportunistic beamforming, user grouping and simplified downlink scheduling," *EprintArxiv*, vol. 59, no. 10, pp. 6441–6463, 2013.

[8] R. D. Taranto, S. Muppirisetty, and R. Raulefs, "Location-aware communications for 5G networks," *IEEE Signal Process. Mag.*, vol. 102, no. 11, pp. 102–112, Aug. 2014.

[9] J. Zhao, H. Xie, F. Gao, W. Jia, S. Jin, and H. Lin, "Time varying channel tracking with spatial and temporal BEM for massive MIMO systems," *IEEE Trans. Wireless Commun.*, vol. 17, no. 8, pp. 5653–5666, Aug. 2018.

[10] S. Dahiya and A. K. Sing, "Channel estimation and channel tracking for correlated block-fading channels in massive MIMO systems," *Digital Commun. Netw.*, vol. 4, no. 2, pp. 138–147, Apr. 2018.

[11] C. Zhang, J. Zhang, Y. Huang, and L. Yang, "Location-aided channel tracking and downlink transmission for HST massive MIMO systems," *IET Commun.*, vol. 11, no. 13, pp. 2082–2088, Oct. 2017.

[12] X. Gao, L. Dai, Y. Zhang, T. Xie, X. Dai, and Z. Wang, "Fast channel tracking for terahertz beamspace massive MIMO systems," *IEEE Trans. Veh. Technol.*, vol. 66, no. 7, pp. 5689–5696, Jul. 2017.

[13] E. Castañeda, A. Silva, and R. Samano-Robles, "Low-complexity user selection for rate maximization in MIMO broadcast channels with downlink beamforming," *Sci. World J.*, vol. 1, no. 2, pp. 865–905, Jan. 2014.

[14] J. Zhao, F. Gao, W. Jia, S. Zhang, S. Jin, and H. Lin, "Angle domain hybrid precoding and channel tracking for millimeter wave massive MIMO systems," *IEEE Trans. Wireless Commun.*, vol. 16, no. 10, pp. 6868–6880, Oct. 2017.

[15] Y. Zhang, D. Wang, J. Wang, and X. You, "Channel estimation for massive MIMO-OFDM systems by tracking the joint angle-delay subspace," *IEEE Access*, vol. 4, pp. 10166–10179, 2016.

[16] D. R. Brown, R. Wang, and S. Dasgupta, "Channel state tracking for large-scale distributed MIMO communication systems," *IEEE Trans. Signal Process.*, vol. 63, no. 10, pp. 2559–2571, May 2015.

[17] Y. Cui and X. Fang, "A massive MIMO-based adaptive multi-stream beamforming scheme for high-speed railway," *Eurasip J. Wireless Commun. Netw.*, vol. 1, no. 1, pp. 1–8, 2015.

[18] Y. Yang, P. Fan, and Y. Huang, "Doppler frequency offsets estimation and diversity reception scheme of high speed railway with multiple antennas on separated carriages," *J. Modern Transp.*, vol. 20, no. 4, pp. 1–6, 2012.

[19] C. Farsakh and J. A. Nossek, "Spatial covariance based downlink beamforming in an SDMA mobile radio system," *IEEE Trans. Commun.*, vol. 46, no. 11, pp. 1497–1506, Nov. 1998.

YANG WANG received the B.S. degree in electronic information engineering and the Ph.D. degree in machinery manufacturing and automation from the Dalian University of Technology, in 1998 and 2003, respectively. He is currently a Professor with the School of Electronic and Communication Engineering, Shenzhen Polytechnic. His interests are in the 5th generation of mobile communication systems and heterogeneous networks communication systems.

YONGXUE WANG received the B.S. degree in measurement and control technology and instrument and the M.S. degree in electric circuit and system from Hunan University, in 1998 and 2001, respectively, and the Ph.D. degree in communication and information systems from the South China University of Technology, in 2006. He is currently an Associate Professor with the School of Electronic and Communication Engineering, Shenzhen Polytechnic. His research interests are in the 5th generation of the mobile communication systems and software-defined networks.

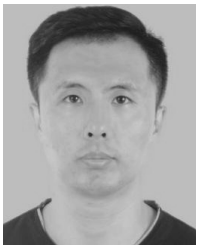

SHENGYU ZHANG received the B.S. degree in electrical engineering and automation and the M.S. degree in power electronics and power drives from the Harbin Institute of Technology, in 2002 and 2005, respectively. He is currently an Associate Professor with the School of Electronic and Communication Engineering, Shenzhen Polytechnic. His research interests are in communication and information systems.

HONGJIE CEN received the B.S. and M.S. degrees from the Wuhan University of Technology, in 2000 and 2003, respectively, all in communication engineering. He is currently a Lecturer with the School of Electronic and Communication Engineering, Shenzhen Polytechnic. His research interests are in communication and information systems.